InGaN/GaN multi-quantum dot light-emitting diodes

L.-W. Ji[a],*, Y.K. Su[a], S.J. Chang[a], C.S. Chang[a], L.W. Wu[a], W.C. Lai[a], X.L. Du[b], H. Chen[b]

[a] *Department of Electrical Engineering, Institute of Microelectronics, National Cheng Kung University, Tainan 701, Taiwan, ROC*
[b] *Institute of Physics, Chinese Academy of Science, Beijing 100080, PR China*

Abstract

It has been demonstrated that InGaN/GaN blue light-emitting diodes (LEDs) with multiple quantum dot (MQD) were successfully fabricated by metal-organic chemical vapor deposition. We have formed nanoscale InGaN self-assembled QDs in the well layers of the active region with a typical 3-nm height and 10-nm lateral dimension. With a 20-mA DC injection current, the forward voltage was 3.1 and 3.5 V for MQD LED and conventional nitride-based multi-quantum well (MQW) LED with the same structure, respectively. It was also found that EL peak position of the MQD LED is more sensitive to the amount of injection current, as compared to the conventional MQW LEDs.
© 2003 Elsevier B.V. All rights reserved.

1. Introduction

Heteroepitaxial growth of highly strained material systems has been quite attractive as it offers the possibility of producing low-dimensional carrier confinement nanostructures, such as quantum wells and self-assembled quantum dots (QDs) [1]. III-nitride semiconductor materials have a wurtzite crystal structure and a direct energy band gap. We could also achieve nitride-based hetero-epitaxial growth easily. At room temperature, the band gap energy of AlInGaN varies from 0.7 to 6.2 eV depends on its composition. Therefore, III-nitride semiconductors are particularly useful for light-emitting diodes (LEDs) and laser diodes (LDs) in this wavelength region [2–5]. Typical high-brightness LEDs have a multiple quantum well (MQW) active region. The MQW LED is a kind of heterojunction device, in which electrons and holes are confined in the well layers. Thus, one can achieve high quantum efficiency from the MQW LEDs since carrier can recombine easily in the confined well layers [6–9]. Although high brightness InGaN/GaN MQW LEDs are already commercially available, we should be able to enhance the LED output intensity by using QDs, instead of MQW, to further confine the carriers.

*Corresponding author. Tel.: +886-6-2757575x6328; fax: +886-6-2351864.

E-mail address: lwji@seed.net.tw (L.-W. Ji).

Recently, it has been shown that nitride nanostructures can be self-organized using the strain-induced Stranski–Krastanov (S–K) growth mode without any substrate patterning process [10–12]. It has also been shown that nitride nanostructures can be self-organized using growth interruption during the metal-organic chemical vapor deposition (MOCVD) growth [13]. Although the size fluctuations of self-assembled QDs could result in inhomogeneous optical and electrical characteristics, the self-assembly of strain-induced islands provides the means for creating zero-dimensional quantum structures without having to overcome the current limitations of lithography. These self-assembled QDs could also be used to study novel device physics [14–16]. In this work, we report the fabrication of blue LEDs with InGaN/GaN multiple quantum dot (MQD) structure. The optical and electrical properties of the InGaN/GaN MQD LEDs will also be reported.

2. Experiment

Samples used in this study were grown on $(0\,0\,0\,1)$-oriented sapphire (Al_2O_3) substrates in a vertical low-pressure MOCVD reactor with a high-speed rotation disk [6–9]. Briefly, the gallium, indium and nitrogen sources were trimethylgallium (TMGa), trimethylindium (TMIn), and ammonia (NH_3), respectively. Biscyclopentadienyl magnesium (CP_2Mg) and disilane (Si_2H_6) were used as the p-type and n-type doping sources, respectively. We first prepared samples with uncapped single layer of InGaN QDs [13]. After a 30-nm-thick low-temperature GaN nucleation layer was deposited onto the sapphire substrate at $500°C$, the temperature was raised to $1000°C$ to grow a 2-μm-thick undoped GaN buffer layer. The growth temperature was then reduced to $730°C$ to grow InGaN QDs with growth rate of 0.04 nm/s. During the deposition of QDs, an interrupted growth method was employed. In other words, we deposited a 1.2-nm-thick InGaN layer on top of the undoped GaN buffer layer, stopped the growth for 12 s, and then deposited another 1.2-nm-thick InGaN layer so as to achieve a total InGaN layer

thickness of 2.4 nm. Room temperature surface morphologies of the InGaN QDs samples were then characterized ex situ by an atomic force microscopy (AFM) system (Shimadzu SPM-9500JZ) with a sharpened Si_3N_4 tip.

In GaN/GaN MQD LEDs were then fabricated. Fig. 1 shows MQD LED structure used in this study. Prior to growth, sapphire substrates were thermally baked at $1100°C$ in hydrogen gas to remove surface contamination. After a 30-nm-thick low-temperature GaN nucleation layer was deposited onto the sapphire substrate at $500°C$, the temperature was raised to $1000°C$ to grow the Si:GaN buffer layer. Subsequently, the temperature was ramped down to $730°C$ to grow the InGaN/GaN MQW active region with InGaN QDs. It should be noted that we introduced interrupted growth method so as to achieve InGaN QD well layers. In other words, we first deposited a 1.2-nm-thick InGaN layer, stopped the growth for 12 s, and then deposited another 1.2-nm-thick InGaN layer so as to achieve a 2.4-nm nominal thickness of InGaN [13]. In the active region, each InGaN/GaN pair consists of a 2.4-nm-thick InGaN QD well layer and a 15-nm-thick GaN barrier layer. The InGaN QD well layers were unintentionally doped. On the other hand, the GaN barrier layers were Si-doped with a doping concentration of $3 \times 10^{17}\,cm^{-3}$ [9]. After growth of active region, the substrate temperature was elevated to $1060°C$ again to grow the Mg-doped AlGaN cladding layer and Mg-doped GaN contact layer. In order to increase the indium
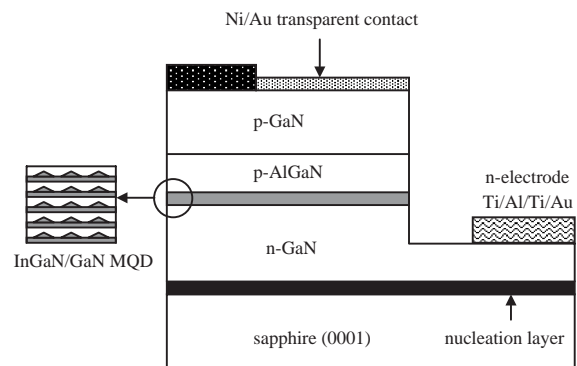
Fig. 1. Schematic structure for the blue LED with InGaN/GaN MQD.

incorporation rate, nitrogen was used as the carrier gas when we grew the InGaN/GaN MQD active regions. On the other hand, hydrogen was used as the carrier gas when we grew other parts of the samples. The growth pressure was kept at 350 mTorr throughout the growth. The as-grown samples were then annealed at 760°C for 25 min in N_2 ambient to activate the Mg-doped p-type layers. With this thermal annealing process, we could achieve uniformly doped highly conductive p-type layers.

For structural characterization, the samples were investigated by high-resolution transmission electron microscopy (HRTEM). Cross sections of these samples along [0 1 $\bar{1}$ 0] wurtzite direction were prepared by mechanical polishing followed by ion milling. TEM observations were performed on a JEM-2010 electron microscope with a Scherzer resolution of 0.19 nm in high-resolution mode. For LED fabrications, we partially etched the surfaces of the p-type layers until the n-type GaN layers were exposed. Ni/Au contacts were subsequently evaporated onto the p-type GaN surfaces to serve as the p-electrodes. On the other hand, Ti/Al/Ti/Au contacts were deposited onto the exposed n-type GaN layers to serve as the n-type electrodes, to complete the fabrication of the blue LEDs. Room temperature electroluminescence (EL) characteristics were then measured by injecting different amount of DC current into the fabricated LEDs on wafer without polishing and package. The current–voltage ($I-V$) measurements were also performed at room temperature by an HP4156 semiconductor parameter analyzer.

3. Results and discussion

Fig. 2(a) shows $500 \times 500 \, \text{nm}^2$ three-dimensional (3-D) AFM image of the sample with uncapped single layer of InGaN QDs. It can be seen clearly from this figure that we could achieve InGaN QDs by growth interruption during MOCVD growth. It was found that the diameter of these QDs was in the range of 20–35 nm, with an average height of 4.0 nm. On the other hand, the density of these QDs was estimated to be around $2 \times 10^{10} \, \text{cm}^{-2}$. Fig. 2(b) shows the cross
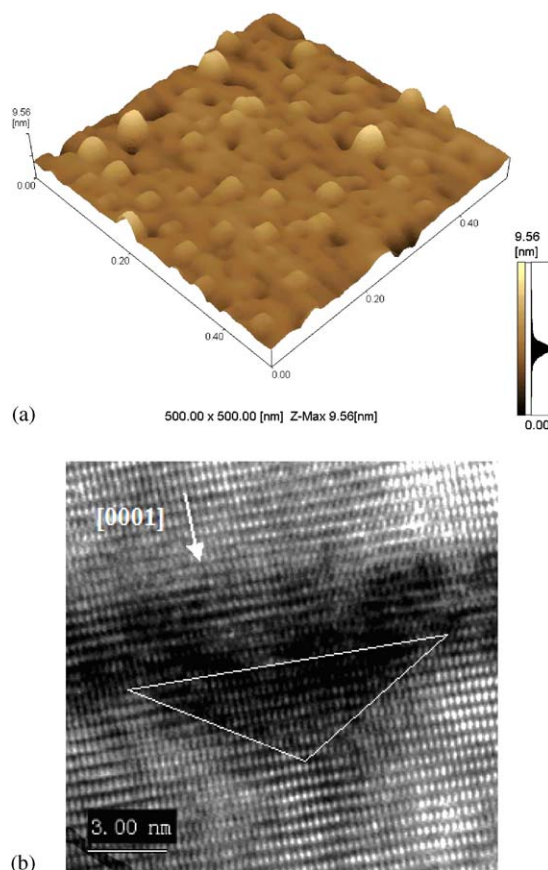
Fig. 2. (a) $500 \times 500 \, \text{nm}^2$ 3-D AFM image of the uncapped QD sample; and (b) HRTEM image, taken along the [0 1 $\bar{1}$ 0] axis, of a SAQD in QW for MQD LED structure, the pyramidal shape of the dot have been outlined.

section HRTEM image for an InGaN QD embedded in InGaN/GaN quantum well of the MQD LED structure. This HRTEM picture reveals that typical dot is pyramidal with a 10 nm diameter and a 3 nm dot height. It should be noted that dot size observed from the HRTEM image of MQD structure (i.e. height/width $= \frac{3}{10}$ nm) seems to be smaller than that observed from the AFM image of uncapped single layer of InGaN QDs, although they were prepared at the same MOCVD growth conditions. This can be understood by the fact that ripening of InGaN QDs for the single layer in the absence of InGaN/GaN stacking layers can enlarge the QD size [17]. Fig. 3 shows $I-V$ characteristics of the MQD LED. With a
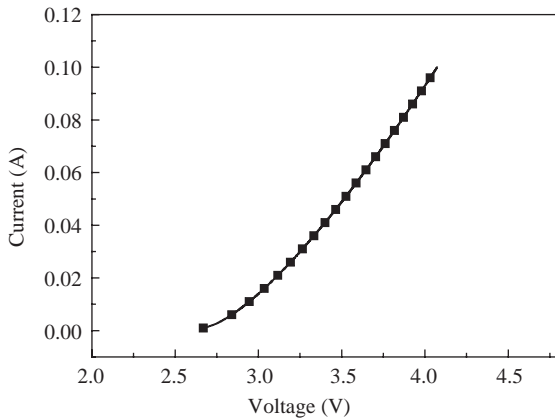
Fig. 3. $I-V$ characteristics of the MQD LED, the forward voltage is 3.1 V at 20-mA injection current.
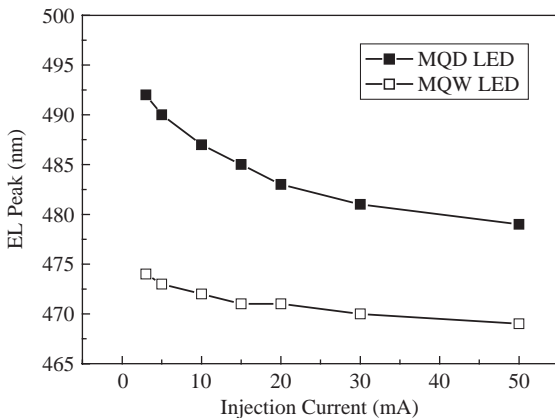
Fig. 4. Dominated wavelength of EL spectra depends on injection current for the MQD LED and conventional MQW LEDs.

20-mA DC injection current, it was found that the forward voltage was only 3.1 V. Such a value is smaller than the 3.5-V forward voltage observed from the conventional nitride-based MQW LED with a similar structure at the same injection current [9]. The smaller 3.1-V forward voltage showing better electrical performance of the fabricated MQD LED, as a result can be attributed to QD is effective in reducing forward voltage due to the 3-D spatial confinement effect of carriers.

Fig. 4 illustrates the EL peak position as a function of injection current for the MQD LED and conventional nitride-based MQW LED with a similar structure [9]. It can be seen that the EL peak position blue shifts toward short wavelength side as the injection current increases. Such a blue shift in EL wavelength could be attributed to the band-filling effect of localized energy states [5,18]. It should be noted that we observed a huge 68.4-meV EL blue shift as the injection current was increased from 3 to 50 mA for the MQD LED. Such a value is much larger than the 38-meV EL blue shift observed from the MQW LED in the same current range [9]. The large EL blue shift reveals that the strain-induced QDs with deep localization of exitons (or carriers) can strengthen band-filling effect as the injection current increases. Hence, the transition energy will become much larger [19,20]. Such a result also suggests that EL peak position of MQD LED is more sensitive to the amount of injection current as compared to conventional MQW LEDs.

4. Conclusion

In summary, InGaN/GaN MQD blue LEDs have been successfully fabricated. With a 12 s growth interruption, we formed nanoscale InGaN self-assembled QDs in the well layers of the active region. It was found that a huge 68.4-meV blue shift in electroluminescence (EL) peak position as the injection current is increased from 3 to 50 mA for the MQD LED. The large EL blue shift reveals that deep localization of exitons (or carriers) originates from QDs will strengthen band-filling effect as the injection current increases.

References

[1] D. Leonard, M. Krinshnamurthy, C.M. Reaves, S.P. Denbaars, P.M. Petroff, Appl. Phys. Lett. 63 (1993) 3203.

[2] S. Nakamura, T. Mukai, M. Senoh, J. Appl. Phys. 76 (1994) 8189.

[3] F.A. Ponce, D.P. Bour, Nature 386 (1997) 351.

[4] I. Akasaki, H. Amano, J. Crystal Growth 175/176 (1997) 29.

[5] S. Nakamura, Science 281 (1998) 956.

[6] Y.K. Su, S.J. Chang, C.H. Ko, J.F. Chen, W.H. Lan, W.J. Lin, Y.T. Cherng, J. Webb, IEEE Tran. Electron. Dev. 49 (2002) 1361.

[7] S.J. Chang, C.H. Kuo, Y.K. Su, L.W. Wu, J.K. Sheu, T.C. Wen, W.C. Lai, J.F. Chen, J.M. Tsai, IEEE J. Sel. Top. Quantum Electron. 8 (2002) 744.

[8] S.J. Chang, W.C. Lai, Y.K. Su, J.F. Chen, C.H. Liu, U.H. Liaw, IEEE J. Sel. Top. Quantum Electron. 8 (2002) 278.

[9] L.W. Wu, S.J. Chang, T.C. Wen, Y.K. Su, W.C. Lai, C.H. Kuo, C.H. Chen, J.K. Sheu, IEEE J. Quantum Electron. 38 (2002) 446.

[10] B. Damilano, N. Grandjean, S. Dalmasso, J. Massies, Appl. Phys. Lett. 75 (1999) 3751.

[11] K. Tachibana, T. Someya, Y. Arakawa, Appl. Phys. Lett. 74 (1999) 383.

[12] C. Adelmann, J. Simon, G. Feuillet, N.T. Pelekanos, B. Daudin, Appl. Phys. Lett. 76 (2000) 1570.

[13] L.W. Ji, Y.K. Su, S.J. Chang, L.W. Wu, T.H. Fang, J.F. Chen, T.Y. Tsai, Q.K. Xue, S.C. Chen, J. Crystal Growth 149 (2003) 144.

[14] S. Nakamura, K. Kitamura, H. Umeya, A. Jia, M. Kobayashi, A. Yoshikawa, M. Shimotomai, Y. Kato, K. Takahashi, Electron. Lett. 34 (1998) 2435.

[15] K. Tachibana, T. Someya, Y. Arakawa, Appl. Phys. Lett. 75 (1999) 2605.

[16] K. Tachibana, T. Someya, Y. Arakawa, IEEE J. Sel. Top. Quantum Electron. 6 (2000) 475.

[17] A. Neogi, H. Everitt, H. Morkoç, T. Kuroda, A. Takeuchi, IEEE Trans. Nonotechnol. 2 (2003) 10.

[18] Y. Narukawa, Y. Kawakami, M. Funato, Sz. Fujita, S. Fujita, S. Nakamura, Appl. Phys. Lett. 70 (1997) 981.

[19] W.R. Tribe, M.J. Steer, D.J. Mowbray, M.S. Skolnick, A.N. Forshaw, J.S. Roberts, G. Hill, M.A. Pate, C.R. Whitehouse, G.M. Williams, Appl. Phys. Lett. 70 (1997) 993.

[20] Y.J. Ding, D.C. Reynolds, S.J. Lee, J.B. Khurgin, W.S. Rabinovich, D.S. Katzer, Appl. Phys. Lett. 71 (1997) 2581.